Comparative Quantum Mechanics/Molecular Mechanics (QM/MM) and Density Functional Theory Calculations on the Oxo−Iron Species of Taurine/α-Ketoglutarate Dioxygenase

Elizabeth Godfrey, Cristina S. Porro, and Sam P. de Visser*

The Manchester Interdisciplinary Biocenter and the School of Chemical Engineering and Analytical Science, The University of Manchester, 131 Princess Street, Manchester M1 7DN, United Kingdom

Received: November 19, 2007; In Final Form: January 7, 2008

We present here the first quantum mechanical/molecular mechanics (QM/MM) studies of taurine/α-ketoglutarate dioxygenase (TauD) enzymes. Our studies are focused on the chemical properties of the oxo−iron species and the effect of the protein environment on its structural and electronic behavior. Although the active site region of TauD is very polar with many key hydrogen bonding interactions and salt bridges, the actual effect of the protein environment on the ordering and relative energies of the possible spin state structures is found to be quite small. Optimized geometries are very close to ones observed with density functional theory models that did not take the protein environment into consideration. The calculations show that protonation of the histidine ligands of iron is essential to reproduce the correct electronic representations of the enzyme. Hydroxylation studies of taurine by the oxo−iron active species predict that it is a very efficient catalyst that reacts with substrates via low reaction barriers.

Introduction

Two classes of enzymes that utilize molecular oxygen on an iron center are dioxygenase and monoxygenase enzymes.[1,2] Dioxygenases use both oxygen atoms of O_2 and donate them to substrate(s), but monoxygenases use only one oxygen atom of O_2 whereas the other oxygen atom leaves the process as water. Another important difference between monoxygenase and dioxygenase enzymes is the fact that dioxygenases lack a cofactor, which makes their application interesting from a biotechnological point of view. A large class of dioxygenase enzymes is the α-ketoglutarate dependent dioxygenases (αKGD) of which taurine/α-ketoglutarate dioxygenase (TauD) is the most thoroughly studied one in that category. These enzymes perform critical tasks in biosystems and have been implicated in the antibiotic fosfomycin biosynthesis, vancomycin synthesis, as well as in herbicide degradation.[3] In addition, in, e.g., humans, AlkB repair enzymes have been shown to belong to the αKGD family and are able to demethylate methylated DNA and RNA bases.[4]

Scheme 1 shows the active site region of the substrates bound complex of *E. coli* TauD as taken from the crystal structure.[5,6] The enzyme has a central iron atom that is linked to the protein backbone through interactions with two histidine (His_{99} and His_{255}) and an aspartic acid (Asp_{101}) side chain. This typical 2His/1Asp motif is a common feature in nonheme enzymes and has been implicated with the activity of the catalyst.[1b,7] In the resting state the remaining three binding sites of iron are occupied with water molecules, but binding of α-ketoglutarate disposes two of those and the third water molecule is expelled when molecular oxygen binds to the iron center. The other substrate (taurine) does not directly bind to the iron center but rather in its vicinity. As can be seen from Scheme 1, taurine due to its polar nature is held in position by a series of strong hydrogen bonding interactions. The sulfonate group of taurine forms a salt bridge with the side chain of Arg_{270} and is also hydrogen bonded to the imidazole side chain of His_{70}. Therefore, the sulfonate group of taurine will be locked in its position and will be quite rigid. The amine group of taurine is located in a more flexible region and forms hydrogen bonds with a nearby crystal water molecule (W). A nearby tyrosinate residue (Tyr_{73}) is locked in hydrogen bonding interactions, with, e.g., an aspartic acid side chain of Asp_{94}. It has been shown that in the absence of taurine substrate a self-hydroxylation reaction converts Tyr_{73} into a catecholate system.[8]

SCHEME 1: Active Site Structure of TauD As Taken from the 1OS7 pdb File[a]

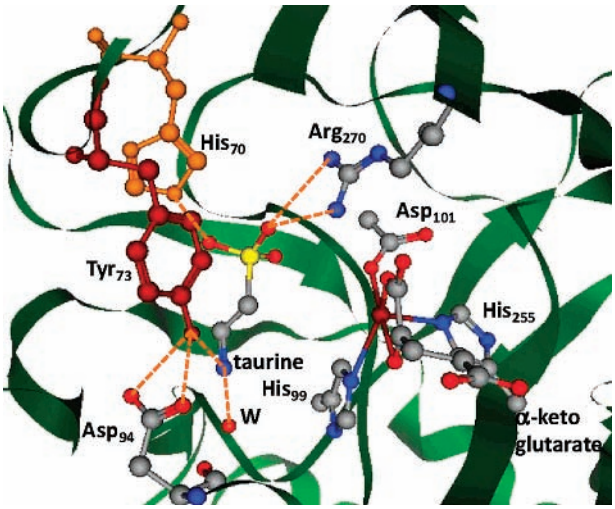

[a] Amino acid residues are labeled according to the pdb file and W is a water molecule.

TauD enzymes undergo a catalytic cycle that starts with binding of the substrate α-ketoglutarate and O_2 to the iron active center, and taurine in its direct neighborhood.[9] At the active center α-ketoglutarate is first oxidized to succinate (Succ) and CO_2 whereby an oxo−iron active species is formed. The oxo−iron species subsequently abstracts a hydrogen atom from taurine and rebounds the hydroxyl group to form products. This oxo−iron (FeO) species has a lifetime that is long enough to be

* Corresponding author. E-mail: sam.devisser@manchester.ac.uk.

10.1021/jp710999v CCC: $40.75
Published on Web 02/01/2008

spectroscopically characterized.[10] Thus, the $^{16}O_2/^{18}O_2$ difference spectrum gave a specific Fe−O vibration at 821 cm^{-1} that downshifted by 34 cm^{-1} after substitution of molecular oxygen with $^{18}O_2$.[10b] Furthermore, Mössbauer studies identified the system as a quintet spin ground state.[10d] Theoretical modeling of the oxo−iron active species of TauD confirmed the catalytic cycle of the enzyme and the spin state identification.[11] These calculations, however, employed small active site models of the enzyme and did not take the protein surrounding into account. To gain insight into the effect of the protein environment on the spin state ordering and optimized geometries of the oxo−iron species of TauD enzymes, we present here the first quantum mechanical/molecular mechanics (QM/MM) studies of TauD and make a direct comparison with small model calculations and published experimental data.

The application of the QM/MM technique to bioinorganic problems has recently been reviewed and shown to be able to accurately reproduce enzymatic systems, although the technique has many pitfalls and difficulties.[12] QM/MM studies on Isopenicillin *N* Synthase showed that the protein perturbs the energetics of the dioxygen binding step by 8−10 kcal mol^{-1} with respect to density functional theory (DFT) calculations on small active site model complexes.[13] In cytochrome P450 enzymes the substrate conformation due to hydrogen bonding interactions was found to be strongly influenced by the protein environment.[14] The electronic properties of the oxo−iron active species of P450 enzymes were found to be extremely sensitive to the protein environment, so that hydrogen bonding interactions toward the cysteinate group changed the system from a thiolate radical into a heme cation radical or vice versa.[15] However, detailed studies of a series of different P450 isozymes showed that all of those had similar charge and spin distributions, so that these spin and charge distributions in the case of the P450s seem to be dependent on the active site atoms and are little influenced by long-range perturbations.[16] Therefore, to find out what the effect of the protein surrounding is on the oxo−iron active species of TauD enzymes, we present here results of a series of QM/MM calculations on this enzyme and give a direct comparison with active site DFT models and experimental data.

Methods

QM/MM Methods. We performed QM/MM calculations on an active site model of TauD using the ONIOM program package as implemented in Gaussian-03.[17,18] We used a two-layer ONIOM whereby the inner layer was treated with UB3LYP/LANL2DZ and the outer layer with a UFF force field.[19−21] In a QM/MM calculation, three energies (E_1, E_2, and E_3) are calculated. Thus, a single point calculation on the inner layer with the MM method gives energy E_1, and a calculation with UB3LYP/LANL2DZ gives energy E_2. Finally, an MM calculation on the complete system produces energy E_3. The total energy of the QM/MM calculation is then

$$E_{QM/MM} = E_2 + E_3 - E_1 \quad (1)$$

All energies referred to in this work are $E_{QM/MM}$ energies and have been corrected for zero-point energies unless specifically notified. Single point calculations using an LACVP** basis set have also been performed and confirmed the spin state ordering.

We started our work from the 1OS7 pdb file,[5] which is a substrates bound crystal structure of *E. coli* TauD, replaced α-ketoglutarate by succinate and added the oxo group to the iron center. Subsequently, hydrogen atoms and solvent water molecules were added and the system was equilibrated. We selected a 56 atom QM region containing the oxo−iron group, taurine, the imidazole groups of His_{99} and His_{255}, acetate for succinate and Asp_{101}, and methylguanidinium for Arg_{270}. All histidine amino acids in the model were in their protonated states unless otherwise mentioned. The border region was described with the link atom approach as implemented in Gaussian. Because Gaussian has a maximum number of atoms for QM/MM calculations of 20 000, we were unable to calculate the complete enzyme monomer plus 15 Å of solvent layer as is commonly done in QM/MM calculations.[15,16] Therefore, we truncated the system to an area containing all amino acids with at least one atom within a 10 Å radius of the transition metal. To prevent the system from undergoing unnatural changes during the geometry optimizations, we fixed all α-carbons except the ones of the amino acids bound to the metal. Full geometry optimizations in default settings followed by an analytical frequency calculation were performed and all structures reported here had real frequencies only. We calculated the oxo−iron species in the lowest lying singlet, triplet, quintet and septet spin states. For the lowest three spin states (triplet, quintet and septet), we subsequently ran geometry scans for the hydrogen abstraction of taurine by the oxo group. This was done by a full geometry optimization with one extra degree of freedom frozen, namely the O−H distance.

DFT Methods. In addition to the QM/MM work, we ran density functional theory (DFT) calculations on model complexes.[22] Full geometry optimizations (without constraints) were initially performed with Jaguar 5.5.[23] Subsequently, the structures were transferred to Gaussian-03, reoptimized and subjected to an analytical frequency calculation. That way, a direct comparison between the QM/MM and DFT models can be made because all calculations use the same optimization procedures and methods. The Jaguar and Gaussian optimized geometries are very similar. The calculations utilized the UB3LYP procedure similarly to the QM/MM work in combination with an LANL2DZ basis set on iron and 6-31G on the rest of the atoms.[19,20] These calculations were performed on an active site model containing oxo−iron, the imidazole groups of His_{99} and His_{255}, acetic acid for succinate and Asp_{101}, carbon dioxide, and substrate propene. No constraints were used in the geometry optimizations.

Results and Discussion

Figure 1 displays optimized geometries and group spin densities of the oxo−iron species of TauD in the quintet, septet, triplet, and singlet spin states as calculated with our QM/MM model, and DFT optimized geometries and group spin densities are shown in Figure 2. On the left-hand-side of Figure 1 we show a 3D-drawing with the QM region highlighted with tubes whereas the dashed amino acids in the background are part of the MM region. The right-hand-side of Figure 1 gives a schematic representation of the active region with critical bond lengths identified. The optimized geometries are close to the ones we obtained before for a small DFT model; cf. Figures 1 and 2.[22] For instance, the small model calculations predicted Fe−O bond lengths of 1.653, 1.785, and 1.906 Å for ^{5}FeO, ^{3}FeO, and ^{7}FeO, respectively, and with QM/MM methods values of 1.656, 1.781, and 1.949 Å were obtained. Similarly, good agreement is also obtained for the $Fe-N_{His99}$, $Fe-N_{His255}$, $Fe-O_{Asp101}$, and $Fe-O_{Succ}$ bond distances; see Figures 1 and 2. Therefore, the extra hydrogen bonding interactions of, e.g., the protons of Arg_{270} with the oxo and succinate groups within the active site pocket have only little effect on the optimized

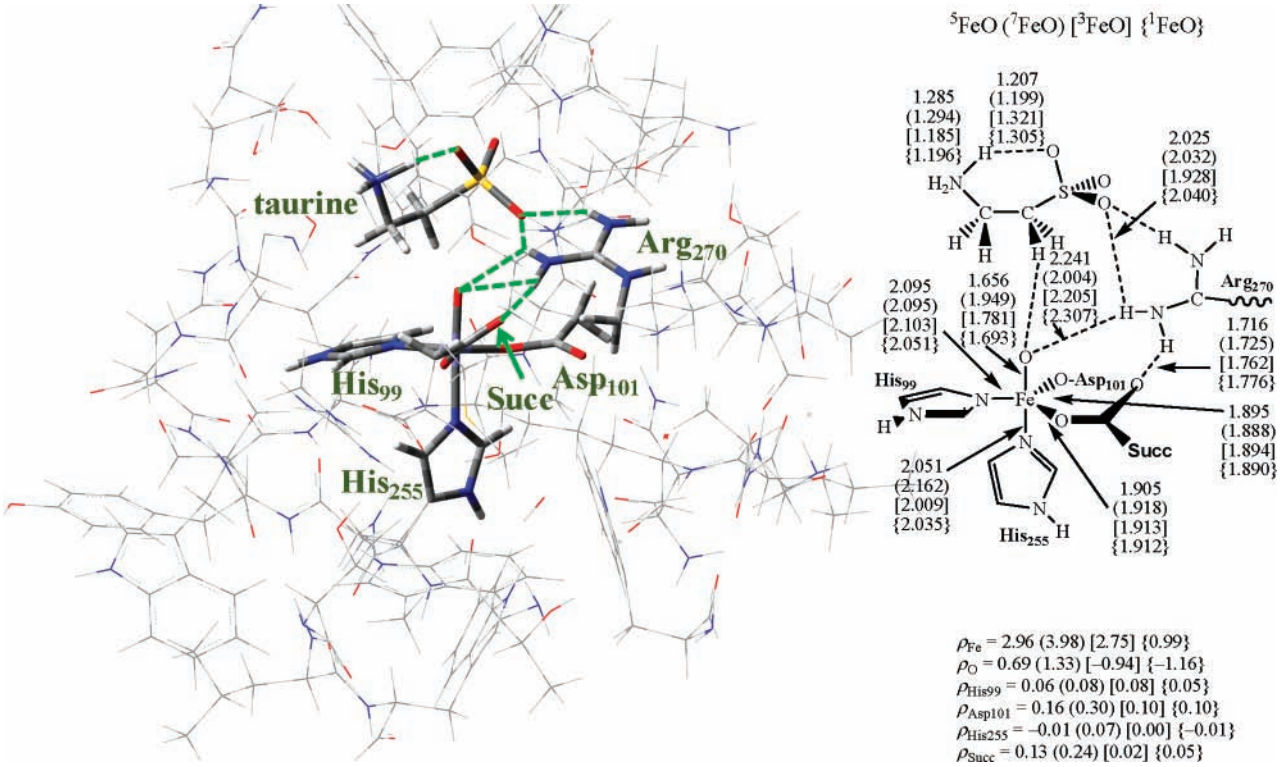

Figure 1. QM/MM optimized geometries of low-lying spin state structures of the oxo−iron species of TauD enzymes. Bond lengths are given in angstroms and group spin densities (ρ) in au.

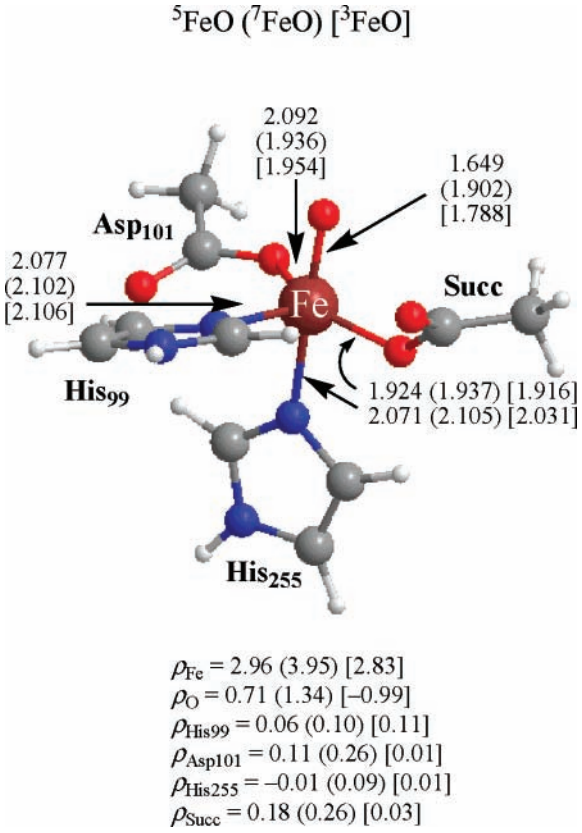

Figure 2. DFT optimized geometries of low-lying spin state structures of the oxo−iron species of TauD enzymes. Bond lengths are given in angstroms and group spin densities (ρ) in au.

geometries of TauD. Moreover, perturbations due to the protein environment do not seem to affect the optimized geometries of the active species of TauD. Note that one of the protons of the amine group of taurine has formed an intramolecular hydrogen bond with one of the oxygen atoms of the sulfonate group. In the quintet and septet spin states this hydrogen atom is located closer to the sulfonate group than to the amine group so that an intramolecular hydrogen atom transfer has taken place. This hydrogen bond is obtained because we did not have a hydrogen bond acceptor in the QM region in the vicinity of the amine group. Nevertheless, the electronic properties of the oxo−iron species are not influenced by this hydrogen bond.

To test the accuracy of our chemical system, we checked the vibrational frequencies and compared those with experimental data from the literature. Thus, Hausinger et al. determined an Fe−O frequency of 821 cm^{-1} for the oxo−iron species.[10b] For other heme and nonheme systems similar values of the Fe−O stretch vibration have been measured.[24] Our frequency calculation of ^{5}FeO predicts this vibrational mode at 849 cm^{-1}, which is somewhat higher than the experimental datum. However, theoretical procedures tend to overestimate vibrational frequencies significantly. Therefore, we scaled this frequency with a factor of 0.9614 as recommended by Scott and Radom for this type of method.[25] A scaled value of 816 cm^{-1} for the Fe−O frequency is then obtained, which is in perfect agreement with the experimentally determined value of Hausinger et al.[10b]

Table 1 gives relative energies of the low lying spin states of the oxo−iron species as obtained with the various methods and techniques. In agreement with previous studies and experimental observations[10d,11,22] the quintet spin structure is the ground state. The septet spin state is higher in energy by 7.6 kcal mol^{-1}, and the triplet and singlet states are 8.3 and 18.9 kcal mol^{-1} above the quintet spin state at the ΔE + ZPE level of theory. These relative energies and spin state orderings are similar to the ones observed for small DFT model complexes, where relative energies of 0.0 (^{5}FeO), 3.8 (^{7}FeO), and 12.1 (^{3}FeO) kcal mol^{-1} were obtained. Therefore, small model complexes reproduce the spin state ordering and the energy differences between the various low-lying states very well.

TABLE 1: Relative Energies of Optimized Geometries of the Oxo−Iron Species of TauD As Calculated with QM/MM or DFT Model Complexes[a]

	QM/MM				DFT	
	$\Delta E_{QM/MM}$[b]	ΔE + ZPE	ΔE_2[c]	$\Delta E_3 - \Delta E_1$[d]	ΔE	ΔE + ZPE
^{1}Fe=O	19.3 (32.2)	18.9	20.9	−1.6	−	−
^{3}Fe=O	9.3 (1.7)	8.3	10.9	−1.6	12.8	12.1
^{5}Fe=O	0.0 (0.0)	0.0	0.0	0.0	0.0	0.0
^{7}Fe=O	8.4	7.6	11.6	−3.2	4.8	3.8

[a] Relative energies in kcal mol^{-1} with respect to ^{5}Fe=O. [b] Values in parentheses obtained with an LACVP** basis set. [c] QM contribution to the relative energy. [d] MM contribution to the relative energy.

To check whether the ordering and relative energies are influenced by the protein environment, we also show the QM energy difference (ΔE_2) and the MM energy difference ($\Delta E_3 - \Delta E_1$) of the total QM/MM energy. Thus, the QM energy difference (ΔE_2) reproduces the spin state ordering of the total $\Delta E_{QM/MM}$. The singlet and triplet spin states are stabilized by only 1.6 kcal mol^{-1} due to the protein environment, and the septet spin state is stabilized by 3.2 kcal mol^{-1}. Therefore, for the description of the oxo−iron species apparently the effect of the protein environment is small as it does not create extra dipole or electrostatic interactions that influence low-lying electronic states. This is in sharp contrast to the cytochromes P450, where an axial bound sulfur atom is involved in hydrogen bonding interactions.[15,26] Inclusion of these hydrogen bonding interactions into the model or through QM/MM changes the electronic properties of the thiolate considerably and changes the system from a sulfur radical into a heme radical. Single point calculations on the oxo−iron species of TauD with an LACVP** basis set stabilize the triplet spin state considerably but the quintet spin state remains the ground state.

In TauD enzymes, all unpaired electrons in the quintet spin state are metal based with occupation: $\pi^*_{x^2-y^2}{}^1\,\pi^*_{xz}{}^1\,\pi^*_{yz}{}^1\,\sigma^*_{xy}{}^1\,\sigma^*_{z^2}{}^0$.[22b,27] The lowest lying orbital of those is the $\pi^*_{x^2-y^2}$ orbital that represents a nonbonding orbital in the plane of His_{99}, Asp_{101}, and succinate. The π^*_{xz} and π^*_{yz} orbitals are the antibonding orbitals along the Fe−O bond and represent combinations of the mixing of a $3d_{xz,yz}$ orbital on iron with $2p_{x,y}$ on the oxygen atom. Finally, the σ^*_{xy} and $\sigma^*_{z^2}$ orbitals give the antibonding interactions of the metal with the His_{99}, Asp_{101} and succinate groups (σ^*_{xy}) or along the O−Fe−His_{255} axis ($\sigma^*_{z^2}$). Although, these orbitals represent interactions of the metal with its ligands, the group spin density on the ligands is small. As a result of that, a stabilizing protein environment has only a minor effect on the group spin densities that are virtually identical in Figures 1 and 2. Furthermore, the oxygen atom of the FeO group in the QM/MM calculations forms a hydrogen bond with two NH groups of Arg_{270}, which we included in our QM region in the QM/MM but left out of our DFT model. This Arg_{270} residue is also involved in hydrogen bonding interactions with the sulfonate group of taurine and therefore is important in the orientation and stability of taurine binding to the active region. Obviously, the behavior of the heme cation radical in heme enzymes is more sensitive to the protein surrounding as the charge and spin is smeared out over a larger surface and because the electron affinities of the heme and cysteinate ligands are different and will affect the group spin densities of heme enzymes.[15,26,28]

As the protein environment around His_{99} does not give a clear indication whether the imidazole group is protonated or not, we ran some additional QM/MM test calculations with the imidazole group of His_{99} deprotonated, while His_{255} was protonated. These calculations were performed using the same model as described above in Figure 1 except for one lesser proton. Full optimizations with ONIOM in the quintet, triplet, and septet spin states were performed. These calculations predicted that the quintet, triplet and septet spin states would be of similar energy: ΔE + $ZPE_{deprotonated\ His99}$ = 0.0 (^{5}FeO), −0.4 (^{3}FeO), and −0.1 (^{7}FeO) kcal mol^{-1}. These relative energies are in contradiction with the systems described above in Figure 1 and with experimental Mössbauer spectra that identified the ground state as a quintet spin state.[10d] Further support that it is unlikely that His_{99} is deprotonated follows from the calculated group spin densities. The group spin densities on the oxo−iron group are similar to the model with protonated His_{99} as shown in Figure 1 with ρ_{Fe} = 2.92 and ρ_O = 0.83. Thus, the charge and spin density on the oxo−iron center is not influenced by the protonation state of one of the ligands bound to iron. However, the calculations show that an electron transfer from Asp_{101} to His_{99} has occurred in the calculations with deprotonated His_{99}, whereby spin densities of ρ_{Asp101} = 1.02 and ρ_{His99} = −0.96 are obtained. Needless to say, at neutral pH, the aspartic acid group should be anionic and deprotonated and contain little spin density. Attempts to swap electrons back to an aspartate anion and neutral histidine failed. Therefore, the system with deprotonated His_{99} is not a realistic representation of the enzyme. Furthermore, these test calculations show that protonation of His_{99} is essential to give the ligand the correct charge and spin distribution and removal of this proton creates an artificial state with a radicalar carboxylic acid group rather than a carboxylate anion. Similar electronic states were obtained for the singlet, septet and triplet spin states. Thus, these test calculations with deprotonated His_{99} show that the choice of the active site region and the protonation state of the various subgroups are crucial for the correct description of the chemical system in QM/MM calculations. As a result of this, we believe that the model with deprotonated His_{99} is not a correct representation of TauD enzymes, but the one with protonated His_{99} is. Therefore, we continued are studies with the model that contains protonated imidazole groups for His_{99} and His_{255}.

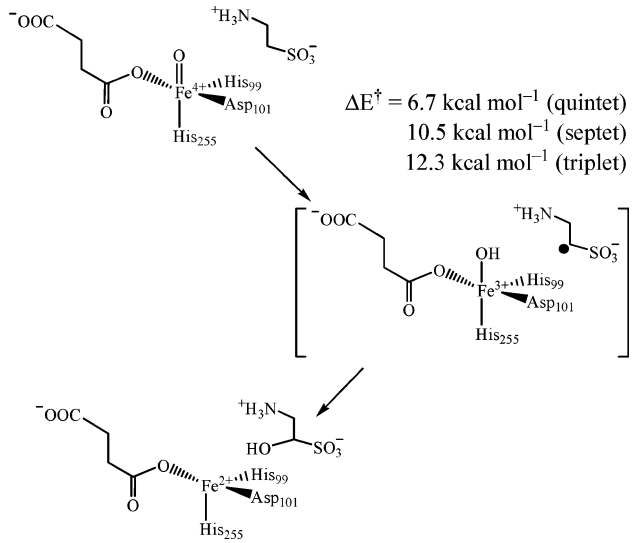

Figure 3. Reaction mechanism of taurine hydroxylation by the oxo−iron species of TauD enzymes as obtained with QM/MM. Energies obtained from geometry scans with fixed O−H distance.

Subsequently, we studied the hydrogen abstraction reaction of taurine by the oxo−iron active species of TauD using the protonated His_{99} model as shown in Figure 1. The results are depicted in Figure 3 and show that the reaction is concerted via an initial hydrogen abstraction barrier (**TS_H**) that directly leads to products. Earlier studies of alkane hydroxylation

reactions by heme and non-heme catalysts showed that these systems generally react via stepwise mechanisms with an initial hydrogen abstraction leading to a radical intermediate followed by hydroxyl rebound to the radical to form hydroxylated products.[29] Nevertheless, with these heme and nonheme systems the rate determining step in the reaction mechanism is also the initial hydrogen abstraction, and because the subsequent barrier leading to products is usually quite small, these intermediates will have a very short lifetime. In the case of the TauD QM/MM work, however, we were unable to locate a stable hydroxyl−iron complex. All attempts to optimize this structure led to formation of a product complex instead. Therefore, it is concluded that the hydroxyl−iron intermediate complex is not a stable intermediate here and immediately collapses to products (Figure 3) and that the reaction proceeds fully concerted. The exothermicity of the overall reaction is 56.8 kcal mol^{-1} in the quintet spin state. This value is in good agreement with DFT calculations of propene hydroxylation by a TauD model where an exothermicity of 52.7 kcal mol^{-1} was obtained. Therefore, the hydrogen abstraction barrier and the reaction exothermicity of QM/MM and DFT models are at par and predict the same conclusion: TauD is a very efficient catalyst of hydrogen abstraction reactions.

Detailed geometry scans (with one degree of freedom fixed, i.e., the O−H distance) predicted hydrogen abstraction barriers of 6.7 (^{5}**TS**$_H$), 10.5 (^{7}**TS**$_H$) and 12.3 (^{3}**TS**$_H$) kcal mol^{-1} for the lowest lying spin states. These barriers are similar to the hydrogen abstraction barrier of the methyl group of propene of 5.4 kcal mol^{-1}, which we observed with the DFT model shown in Figure 2.[22b] Consequently, the protein environment in TauD enzymes has only a small effect on the reaction mechanism and chemical properties of the active species of TauD. The conclusions drawn from model calculations are supported by QM/MM and show that the oxo−iron active species of TauD enzymes is an extremely efficient oxidant that can abstract hydrogen atoms of substrates with very low barriers. These barriers are significantly lower than ones observed for the oxo−iron species of P450 enzyme models and QM/MM.[15,29,30]

Conclusion

In summary, comparative DFT and QM/MM calculations on the oxo−iron species of TauD enzymes have been performed. Generally, the DFT optimized geometries and electronic properties are reproduced with QM/MM. The effect of the protein surrounding is found to be very small, although the protonation state of His$_{99}$ is found to be crucial for a correct description of the active species. Geometry scans reveal that the oxo−iron species of TauD is an efficient oxidant of hydroxylation reactions, as already predicted with DFT models.

Acknowledgment. The National Service of Computational Chemistry Software (NSCCS) and the University of Manchester are acknowledged for providing CPU time. C.S.P. acknowledges DTA for a Ph.D. studentship.

Supporting Information Available: Cartesian coordinates of all structures described in this work and reference 18 in full are available free of charge via the Internet at http://pubs.acs.org.

References and Notes

(1) (a) Ryle, M. J.; Hausinger, R. P. *Curr. Opin. Chem. Biol.* **2002**, *6*, 193−201. (b) Costas, M.; Mehn, M. P.; Jensen, M. P.; Que, L., Jr. *Chem. Rev.* **2004**, *104*, 939−986. (c) Abu-Omar, M. M.; Loaiza, A.; Hontzeas, N. *Chem. Rev.* **2005**, *105*, 2227−2252.

(2) (a) Sono, M.; Roach, M. P.; Coulter, E. D.; Dawson, J. H. *Chem. Rev.* **1996**, *96*, 2841−2887. (b) Ortiz de Montellano, P. R., Ed. *Cytochrome P450: Structure, Mechanism and Biochemistry*, 3rd ed.; Kluwer Academic/Plenum Publishers: New York, 2004. (c) Groves, J. T. *J. Inorg. Biochem.* **2006**, *100*, 434−447. (d) Meunier, B.; de Visser, S. P.; Shaik, S. *Chem. Rev.* **2004**, *104*, 3947−3980.

(3) (a) Higgins, L. J.; Yan, F.; Liu, P.; Liu, H.-W.; Drennan, C. L. *Nature* **2005**, *437*, 838−844. (b) Choroba, O. W.; Williams, D. H.; Spencer, J. B. *J. Am. Chem. Soc.* **2000**, *122*, 5389−5390. (c) Fukumori, F.; Hausinger, R. P. *J. Biol. Chem.* **1993**, *268*, 24311−24317.

(4) Mishina, Y.; Duguid, E. M.; He, C. *Chem. Rev.* **2006**, *106*, 215−232.

(5) O'Brien, J. R.; Schuller, D. J.; Yang, V. S.; Dillard, B. D.; Lanzilotta, W. N. *Biochemistry* **2003**, *42*, 5547−5554 .

(6) Berman, H. M.; Westbrook, J.; Feng, Z.; Gilliland, G.; Bhat, T. N.; Weissig, H.; Shindyalov, I. N.; Bourne, P. E. *Nucl. Acids Res.* **2000**, *28*, 235−242.

(7) (a) Hegg, E. L.; Que, L. Jr. *Eur. J. Biochem.* **1997**, *250*, 625−629. (b) Que, L., Jr. *Nat. Struct. Biol.* **2000**, *7*, 182−184. (c) Que Jr. L. *Acc. Chem. Res.* **2007**, *40*, 493−500. (d) Nam, W. *Acc. Chem. Res.* **2007**, *40*, 522−531.

(8) Koehntop, K. D.; Marimanikkuppam, S.; Ryle, M. J.; Hausinger, R. P.; Que, L., Jr. *J. Biol. Inorg. Chem.* **2006**, *11*, 63−72.

(9) (a) Bollinger, J. M., Jr.; Price, J. C.; Hoffart, L. M.; Barr, E. W.; Krebs, C. *Eur. J. Inorg. Chem.* **2005**, 4245−4254. (b) Bollinger, J. M., Jr.; Krebs, C. *J. Inorg. Biochem.* **2006**, *100*, 586−605. (c) Krebs, C.; Fujimori, D. G.; Walsh, C. T.; Bollinger, J. M., Jr. *Acc. Chem. Res.* **2007**, *40*, 484−492.

(10) (a) Price, J. C.; Barr, E. W.; Tirupati, B.; Bollinger, J. M., Jr.; Krebs, C. *Biochemistry* **2003**, *42*, 7497−7508. (b) Proshlyakov, D. A.; Henshaw, T. F.; Monterosso, G. R.; Ryle, M. J.; Hausinger, R. P. *J. Am. Chem. Soc.* **2004**, *126*, 1022−1023. (c) Riggs-Gelasco, P. J.; Price, J. C.; Guyer, R. B.; Brehm, J. H.; Barr, E. W.; Bollinger, J. M., Jr.; Krebs, C. *J. Am. Chem. Soc.* **2004**, *126*, 8108−8109. (d) Krebs, C.; Price, J. C.; Baldwin, J.; Saleh, L.; Green, M. T.; Bollinger, J. M., Jr. *Inorg. Chem.* **2005**, *44*, 742−757.

(11) (a) Borowski, T.; Bassan, A.; Siegbahn, P. E. M. *Chem. Eur. J.* **2004**, *10*, 1031−1041. (b) Sinnecker, S.; Svensen, N.; Barr, E. W.; Ye, S.; Bollinger, J. M., Jr.; Neese, F.; Krebs, C. *J. Am. Chem. Soc.* **2007**, *129*, 6168−6179.

(12) (a) Senn, H. M.; Thiel, W. *Curr. Opin. Chem. Biol.* **2007**, *11*, 182−187. (b) Senn, H. M.; Thiel, W. *Top. Curr. Chem.* **2007**, *268*, 173−290. (c) Kirchner, B.; Wennmohs, F.; Ye, S.; Neese, F. *Curr. Opin. Chem. Biol.* **2007**, *11*, 134−141.

(13) Lundberg, M.; Morokuma, K. *J. Phys. Chem. B* **2007**, *111*, 9380−9389.

(14) Swart, M.; Groenhof, A. R.; Ehlers, A. W.; Lammertsma, K. *Chem. Phys. Lett.* **2005**, *403*, 35−41.

(15) Schöneboom, J. C.; Lin, H.; Reuter, N.; Thiel, W.; Cohen, S.; Ogliaro, F.; Shaik, S. *J. Am. Chem. Soc.* **2002**, *124*, 8142−8151.

(16) Bathelt, C. M.; Zurek, J.; Mulholland, A. J.; Harvey, J. N. *J. Am. Chem. Soc.* **2005**, *127*, 12900−12908.

(17) (a) Maseras, F.; Morokuma, K. *J. Comput. Chem.* **1995**, *16*, 1170−1179. (b) Vreven, T.; Byun, K. S.; Koma'romi, I.; Dapprich, S.; Montgomery, J. A., Jr.; Morokuma, K.; Frisch, M. J. *J. Chem. Theory Comput.* **2006**, *2*, 815−826.

(18) Frisch, M. J.; et al. *Gaussian 03*, revision C.01; Gaussian Inc.: Wallingford, CT, 2004.

(19) (a) Becke, A. D. *J. Chem. Phys.* **1993**, *98*, 5648−5652. (b) Lee, C.; Yang, W.; Parr, R. G. *Phys. Rev. B* **1988**, *37*, 785−789.

(20) Hay, P. J.; Wadt, W. R. *J. Chem. Phys.* **1985**, *82*, 299−310.

(21) Rappé, A. K.; Casewit, C. J.; Colwell, K. S.; Goddard, W. A., III; Skiff, W. M. *J. Am. Chem. Soc.* **1992**, *114*, 10024−10035.

(22) (a) de Visser, S. P. *Angew. Chem., Int. Ed.* **2006**, *45*, 1790−1793. (b) de Visser, S. P. *J. Am. Chem. Soc.* **2006**, *128*, 9813−9824. (c) de Visser, S. P. *Chem. Commun.* **2007**, 171−173. (d) Aluri, S.; de Visser, S. P. *J. Am. Chem. Soc.* **2007**, *129*, 14846−14847.

(23) *Jaguar 5.5*; Schrödinger, LLC: Portland, OR, 2003.

(24) (a) Ghosh, A.; Almlöf, J.; Que, L, Jr.. *J. Phys. Chem.* **1994**, *98*, 5576−5579. (b) Green, M. T. *J. Am. Chem. Soc.* **2006**, *128*, 1902−1906.

(25) Scott, A. P.; Radom, L. *J. Phys. Chem.* **1996**, *100*, 16502−16513.

(26) (a) Ogliaro, F.; Cohen, S.; de Visser, S. P.; Shaik, S. *J. Am. Chem. Soc.* **2000**, *122*, 12892−12893. (b) de Visser, S. P.; Shaik, S.; Sharma, P. K.; Kumar, D.; Thiel, W. *J. Am. Chem. Soc.* **2003**, *125*, 15779−15788.

(27) Decker, A.; Solomon, E. I. *Curr. Opin. Chem. Biol.* **2005**, *9*, 152−163.

(28) de Visser, S. P.; Shaik, S. *J. Am. Chem. Soc.* **2003**, *125*, 7413−7424.

(29) (a) de Visser, S. P.; Kumar, D.; Cohen, S.; Shacham, R.; Shaik, S. *J. Am. Chem. Soc.* **2004**, *126*, 8362−8363. (b) Shaik, S.; Kumar, D.; de Visser, S. P.; Altun, A.; Thiel, W. *Chem. Rev.* **2005**, *105*, 2279−2328. (c) de Visser, S. P. *J. Am. Chem. Soc.* **2006**, *128*, 15809−15818.

(30) (a) Schöneboom, J. C.; Neese, F.; Thiel, W. *J. Am. Chem. Soc.* **2005**, *127*, 5840−5853. (b) Altun, A.; Shaik, S.; Thiel, W. *J. Am. Chem. Soc.* **2007**, *129*, 8978−8987.